Differentiating Series and Parallel Photovoltaic Arc-Faults

Jay Johnson[1], Michael Montoya[1], Scott McCalmont[2], Gil Katzir[2], Felipe Fuks[2],
Justis Earle[2], Armando Fresquez[1], Sigifredo Gonzalez[1], and Jennifer Granata[1]
[1]Sandia National Laboratories, Albuquerque, NM, 87185, USA
[2]Tigo Energy, Los Gatos, CA, 95032, USA

***Abstract* — The 2011 *National Electrical Code*® requires PV DC series arc-fault protection but does not require parallel arc-fault protection. As a result, manufacturers are creating arc-fault circuit interrupters (AFCIs) which only safely de-energize the arcing circuit when a series arc-fault occurs. Since AFCI devices often use the broadband AC noise on the DC side of the PV system for detection and series and parallel arc-faults create similar frequency content, it is likely an AFCI device will open in the event of either arc-fault type. In the case of parallel arc-faults, opening the AFCI will not extinguish the arc and may make the arc worse, potentially creating a fire. Due to the fire risk from parallel arc-faults, Tigo Energy and Sandia National Laboratories studied series and parallel arc-faults and confirmed the noise signatures from the two arc-faults types are nearly identical. As a result, three alternative methods for differentiating parallel and series arc-faults are presented along with suggestions for arc-fault mitigation of each arc-fault type.**

***Index Terms* — photovoltaic systems, arc-fault detection, series and parallel arc-faults, sensors, monitoring, power system safety**

I. INTRODUCTION

The 2011 *National Electrical Code*® (*NEC*) [1] requires series arc-fault protection, but does not require parallel arc-fault detection or mitigation. Series arc-faults are created when there is a discontinuity in a conductor and the current bridges this gap. Parallel arc-faults are created when an arc is established between conductors at different potentials. Though there are many potential parallel arc-fault paths, three generic types of parallel arc-faults are shown in Figure 1. These parallel arc-faults include:

1. *Parallel Arc-Fault to Grounded Conductor* – This parallel arc-fault could result from the negative DC cable (often grounded in the USA) shorting to a positive conductor due to wear, rodent bites, or damage to cables in conduit runs. In the case of the Mount Holly, NC fire [2] and the Bakersfield, CA fire [3], the fault path was established through the grounded current-carrying conductor via two faults to the conduit.
2. *Cross-String Parallel Arc-Fault* – This fault occurs when conductors on different strings at different potentials arc.
3. *Intra-String Parallel Arc-Fault* – This parallel arc-fault can occur anywhere in the string where a short occurs, e.g., in junction boxes [4].

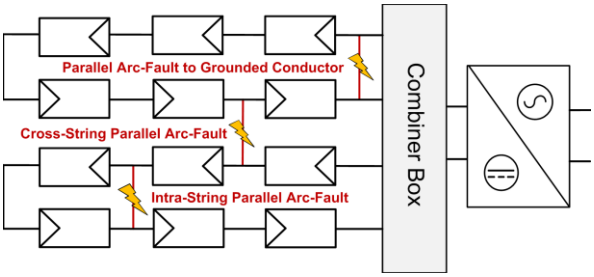

Fig. 1. Different types of parallel arc-faults on the DC side of a PV array.

Currently a number of companies are developing series arc-fault protection devices [5-6]. Many Arc-Fault Circuit Interrupters (AFCIs) use elevated AC noise on the DC side of the PV system to detect series arc-faults. The difficulty comes in differentiating series and parallel arc-faults because the noise signatures are similar. Additionally, many AFCIs are designed to be installed at the string or array-level [7] so if a parallel arc-fault causes the AFCI to trip, the arc will not be extinguished and may strengthen as more current is directed through the arc-fault path. As a result, it is imperative that AFCIs make the appropriate corrective action when an arc-fault occurs.

At this point, there is no consensus on a method for determining which type of arc-fault is present in the PV system. Strobl and Meckler proposed that parallel arc-faults could be identified by the large change in current [8]. However, it may be difficult to differentiate shading from a fast moving cloud or plane from a parallel arc-fault if the current is monitored alone. Another option may be to use the voltage to identify parallel arc-faults, but in the case of intra-string parallel arc-faults across a single module, this change in voltage would be no different from one bypass diode engaging.

Other questions exist about how to effectively extinguish parallel arc-faults. Häberlin proposed to have the AFCI open the string to extinguish the series arc-fault, then, if the arcing frequencies still exist, short the string to extinguish the parallel arc-fault [9]. This methodology would prevent most parallel arc-faults, but special attention would need to be paid to the case of cross-string parallel arc-faults because both strings must be shorted. SMA has recommended isolation monitoring to prevent parallel faults [10], but they believe module-level shorting is required to stop a parallel arc-fault [11]. Johnson

also suggested shorting the modules when parallel arc-faults were identified [6], although this still leaves the system energized at the maximum current (I_{sc}) until night—or otherwise shaded—when the defective components can be replaced.

The goal of this work is to identify electrical conditions which differentiate parallel and series arc-faults and to suggest a prevention methodology for incorporation into arc-fault circuit protection tools. First, we model different parallel arc-faults using single diode module models. These models show a need for experimental analysis as accurate simulations of the system with arc-faults is difficult. Experiments were performed with Tigo Energy at the Distributed Energy Technologies Laboratory (DETL) at Sandia National Laboratories using Tigo Energy's Arc-Fault Detector (AFD). Though designed specifically for series arc-faults, the AFD detected parallel and series arc-faults because the frequency content of the different arc-fault types were nearly identical. Lastly, we present three methods for differentiating series and parallel arc-faults and suggest appropriate actions to mitigate the risk of electrical fires from parallel arc-faults.

II. PARALLEL ARC-FAULT MODEL

Modeling the effect of a parallel arc-fault on a PV string is challenging because of the variability in location, strength, and duration of the arc-fault. Using a standard single diode PV model [12] and basic inverter model [13], the effects of the different parallel arc-faults were studied. We assume the modules have bypass diodes, and operate at V_{MPP} = 50 V and I_{MPP} = 3 A, and the inverter acts as a resistive load operating at the maximum power point (MPP) with effective resistance of 60 Ω. (We later show this inverter model captures the behavior of a load bank well but is insufficient for arc-faults with an inverter.)

For a parallel arc-fault to the grounded conductor, shown in Fig. 1, the PV string current is split between the inverter and the arc-fault path. The parallel arc-fault is fed differently depending on the inverter components, topology, MPP tracking (MPPT) algorithm, module I-V curves, and the arc-fault impedance. The current is divided between the inverter and arc resistances according to,

$$i_{MPP} = i_{inverter} + i_{arc} = \frac{6 \cdot V_{MPP}}{R_{inverter}} + \frac{6 \cdot V_{MPP}}{R_{arc}} \quad (1)$$

where $R_{inverter}$ is the effective MPP resistance of the inverter and R_{arc} is the arc resistance. The exact division of current is difficult to predict, as the arc resistance is nonlinear and dependent on gap length, electrode material, arc current, and electrode geometry [14]. During this parallel arc-fault case, since R_{arc} is generally smaller than $R_{inverter}$, monitoring the current change at the inverter would detect the arc-fault. Note that this is the only test case required for Type 2 devices (parallel arc-fault detectors) in UL Subject 1699B [15].

If a cross-string parallel arc-fault occurred as shown in Fig. 2, the arc current and power would be determined by the arc resistance. The 200 V drop across the arc-fault path means the arc-fault would initiate with a shorter conductor gap compared to the fault across the entire string.

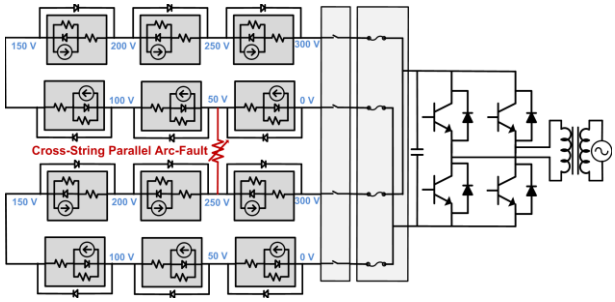

Fig. 2. Circuit model of cross-string parallel arc-fault with MPP voltages.

During an intra-string parallel arc-fault, a portion of the current will pass through the arc-fault path from the higher to lower voltage potentials in the string based on the resistance of the arc-fault. Based on the complex arc-fault and system interactions, experimental tests were conducted to better understand each of these parallel arc-fault cases.

III. ARC-FAULT TESTING

As discussed above, the electrical behavior of parallel arc-faults are highly dependent on the PV system and nature of the arc path. In order to better understand this phenomenon, a series of arc-fault tests were performed at DETL.

A. Experimental Test Setup

Testing was completed on two strings of six or seven 200 W crystalline Si modules and a 3 kW inverter. The data acquisition system, shown in Fig. 3, consisted of a Fluke 87 voltmeter and Tektronix DCM910 current meter to measure the arc-fault voltage and current, a Empro 20A:100mV shunt and Tektronix P5200 differential voltage probe to measure the array current and voltage, and a Pearson 110A current transformer connected to National Instruments PXI-5922 digi-

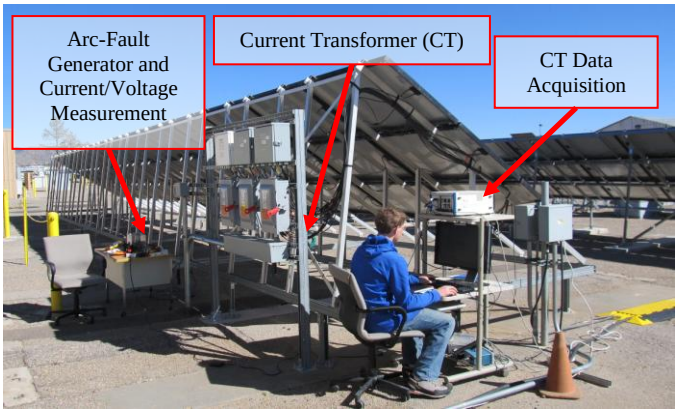

Fig. 3. Experimental setup and instrumentation.

tizer to perform real-time FFT measurements of string current, monitor inverter and arcing noise, and record noise signatures. The arc-fault generator (AFG) [7] was installed between modules using MC4 T-branch connectors.

B. Series Arc-Faults

Series arc-faults occur in the electrical circuit of the PV system due to corrosion or other conductor discontinuities. Series arc-faults differ from parallel arc-faults in that the string current and voltage only vary slightly from normal operation [6] and the location of the arc-fault also does not change the string current or voltage, shown in Fig. 4. The Tigo Energy AFD was tested for series arc-fault detection on multiple inverters and using a load bank. One test with the trip signal is shown in Fig. 5.

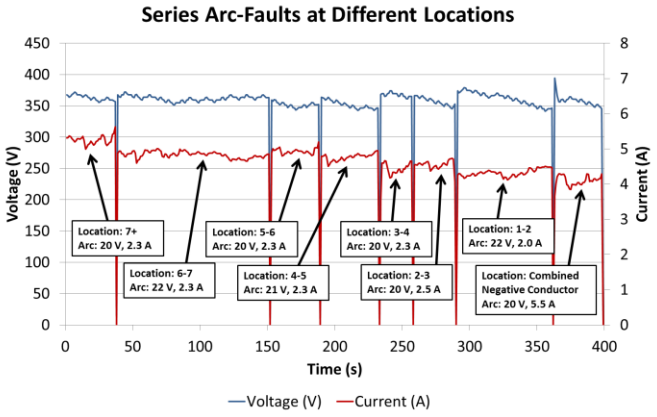

Fig. 4. Series arc-faults at different locations with an inverter. The current drift over the test is due to decreasing irradiance. For the locations, "7+" refers to the positive conductor of the 7th module counted from the grounded negative DC conductor. "5-6" refers to an arc-fault generated between modules 5 and 6.

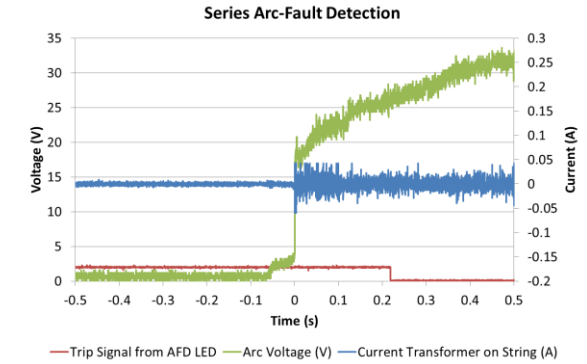

Fig. 5. Example data from a series arc-fault test showing 219 ms trip time.

During testing, generating arc-faults with the load bank was not challenging, however generating arc-faults with the inverter was difficult if string lengths were not sufficient. Series arc-faults could not be sustained using a 3 kW inverter with two strings of six modules, but with 7-module strings, arcs were repeatedly drawn by separating two Cu electrodes. The ignition difficulty in the smaller system was because the maximum voltage available to the arc is V_{oc} minus V_{mpp} since the DC smoothing capacitor in the inverter is charged to V_{mpp}. Thus, if the voltage drop over the arc-fault gap becomes greater than V_{oc} - V_{mpp} the faulted string reaches V_{oc} and there is no long any string current. The dielectric strength of air is large until the arc ionizes the atmosphere, so by using the hand-operated arc-fault generator, the gap tolerance could not be controlled well enough to establish the arc with six modules per string. As a result, it is possible that for some inverters the input capacitor could act as a series arc-fault protection device.

C. Parallel Arc-Faults

Parallel arc-fault tests were completed with a resistive load bank and with an inverter. The load bank resistance was set to near the maximum power point (MPP) of two parallel strings of six modules. Parallel arc-faults to the grounded conductor, intra-string, and cross-string parallel arc-faults were generated. The Fast Fourier Transform (FFT) of the DC line current from 0-100 kHz with a Hanning window is shown in Fig. 6. The noise generated by the different parallel arc-faults and a series arc-fault (black trace) are similar. It is unlikely that an arc-fault detector would be able to differentiate series and parallel arc-faults sensing current frequencies alone.

As described in Section II, the parallel arc-fault establishes a 2nd current loop in the PV system, so a portion of the PV power passes through the parallel arc-fault as opposed to the load bank or inverter. As shown in the 1-second data in Fig. 7, the percentage of this current and voltage is dependent on the location of the parallel arc-fault. Fig. 7 also shows that the resistance of the arc-fault is much smaller than the load bank because nearly all of the current passes through the low resistance arc-fault path. This closely matches the behavior described by Eq. (1) when $R_{arc} << R_{inverter}$.

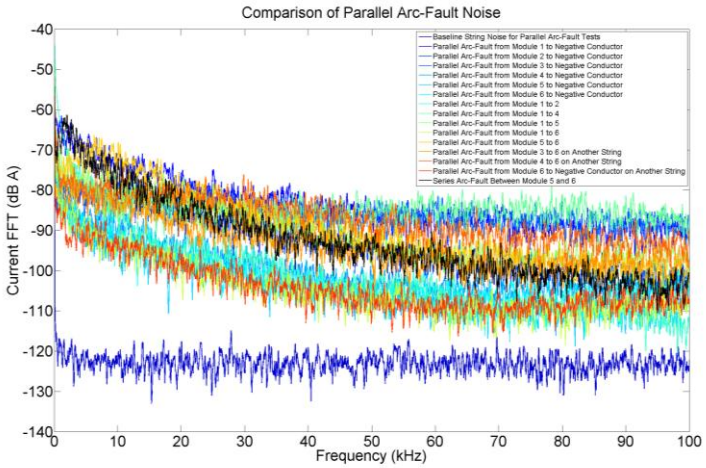

Fig. 6. Different parallel arc-fault noise signatures compared to a series arc-fault. Data are smoothed with 800 Hz rectangular-sliding average.

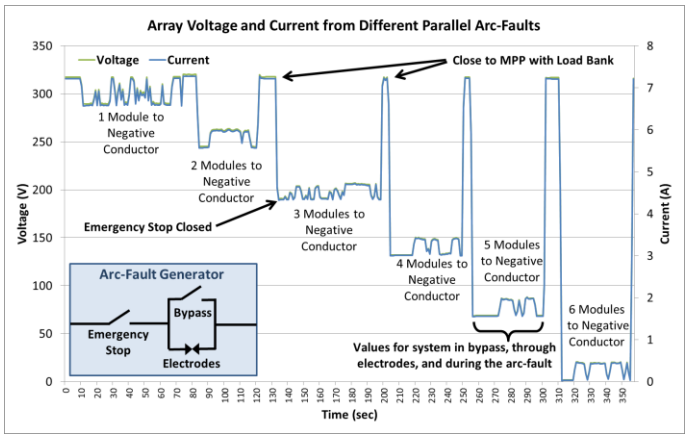

Fig. 7. Current and voltage changes at the load bank due to parallel arc-faults.

In Table I, the system currents and voltages are shown for various parallel arc-faults. Connections to the modules were made at the positive conductor. The load bank current and voltage (I_{LB}, V_{LB}) are given as the range of values during AFG bypass, conduction through the electrodes, and during the arc-fault. The larger values are at the time of the sustained arc-fault. As seen in the table, the arc voltage is consistent for all the cases because the arc-gap was nearly the same for all the tests. Increasing the gap would have increased the arc voltage and produced higher levels of AC noise on the system. The arc-fault path has low impedance compared to the load bank so nearly all the available current travels through the arc-fault. Thus, the current through the arc-fault is principally dependent on the number of modules that are shorted, regardless of the type of parallel arc-fault. The remaining PV-generated current passes through the load bank and the voltage drop across the load is related proportionally by Ohm's law.

TABLE I. ARC AND LOAD BANK CURRENT AND VOLTAGE VALUES DURING DIFFERENT PARALLEL ARC-FAULTS

	V_{arc} (V)	I_{arc} (A)	V_{LB} (V)	I_{LB} (A)
Near MPP without Arc-Fault	0	0	317	7.2
Module 1 to Negative Conductor	*	*	289-317	6.6-7.2
Module 2 to Negative Conductor	22	2.4	245-262	5.5-6.0
Module 3 to Negative Conductor	18	3.7	191-206	4.4-4.7
Module 4 to Negative Conductor	18	5.0	132-150	3.0-3.4
Module 5 to Negative Conductor	18	6.5	67-87	1.6-2.0
Module 6 to Negative Conductor	18	8.1	0-20	0.0-0.5
Module 1 to Module 2	*	*	288-314	6.5-7.1
Module 1 to Module 3	22	1.8	243-261	5.5-5.9
Module 1 to Module 4	20	3.3	191-208	4.3-4.7
Module 1 to Module 5	18	4.8	130-154	3.0-3.5
Module 1 to Module 6	20	6.1	68-87	1.5-2.0
Module 5 to Module 6	*	*	284-310	6.5-7.0
Module 3 to Module 6 on 2nd String	20	4.6	133-151	3.0-3.4
Module 4 to Module 6 on 2nd String	20	3.3	187-207	4.3-4.7

* Unsustained or sputtering arc-fault.

Parallel arc-faults were also generated on two strings of seven modules with a 3 kW high frequency inverter. In these tests, the string conductors were joined with T-branch connectors before the DC disconnect. The configuration created a conductive loop which acted as an antenna and also allowed baseline and arc-fault noise to propagate in the array with DC disconnect open. As a result, there were more spikes in the baseline spectrum between 0-300 kHz and, when the inverter was running, there was noise at the switching frequency and its harmonics, shown in Fig. 8. As with the resistive load bank tests, the parallel and series arc-fault noise were similar. The parallel arc-fault from Module 7 to the negative conductor was not performed because shorting the input capacitor to the inverter was believed to be potentially dangerous.

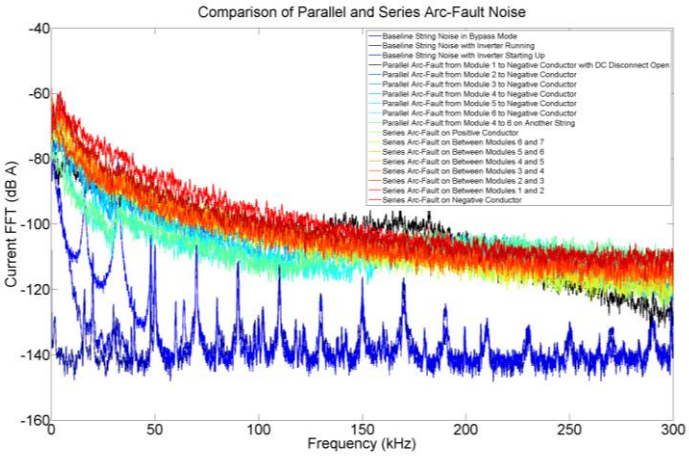

Fig. 8. FFT of string current during parallel and series arc-faults with a 3 kW inverter. Data smoothed with 400 Hz rectangular sliding-average.

The string current and voltage during the inverter test cases were completely different than those presented in Table I. As shown in Fig. 9, the voltage across the inverter was related to the number of modules that were shorted by the arc-fault path, similar to the load bank tests. However, in all cases, the current to the inverter dropped to zero when parallel arc-faults were generated. This may be a result of the test sequence: the electrodes were briefly touched together and then quickly separated to establish the parallel arc-fault. This is different than the UL 1699B standard which uses steel wool to create the parallel arc-fault. By closing the electrodes very briefly, the string becomes shorted and the inverter may stop operating. This was the case except in the 1st *Ground to 4+* arc-fault in Fig. 9. Another reason the inverter may turn off during parallel arc-faults is there is little or no current reaching the inverter. Each module was rated at I_{sc} = 3.8 A and I_{mmp} = 3.5 A, but for all parallel arc-fault tests listed in Fig. 7, the current through the arc fault was nearly $2I_{sc}$ (4.4-6.3 A depending on the time of day) meaning the 2nd string was back-feeding the parallel arc-fault through the bypass diodes and the current path no longer included the inverter. Further testing is required to determine if this is the case for all parallel arc-faults with an inverter running. Different array configurations (i.e., single string, multiple stings) should also be tested.

Unfortunately, when the inverter shuts off during a parallel arc-fault, it does not extinguish the arc-fault. Instead the arc remains energized until the current flow stops, the arc self-

extinguishes by burning through the electrodes, or appropriate action is taken by a "Type 2" AFCI. Parallel arc-faults were detected by the Tigo Energy AFD and tripped within 170-450 ms for the tests conducted at DETL, indicating arc-fault detection of parallel arc-faults is possible. One example of Tigo Energy's AFD performing parallel arc-fault detection is shown in Fig. 10.

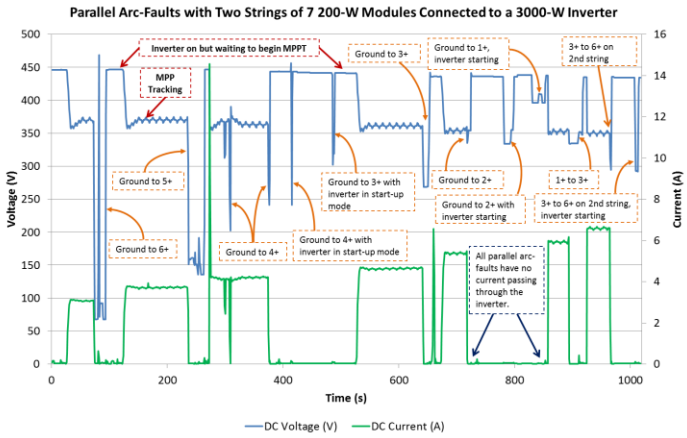

Fig. 9. Parallel arc-fault current and voltage data at the inverter. "Ground" refers to the grounded current-carrying conductor (the negative DC string conductor).

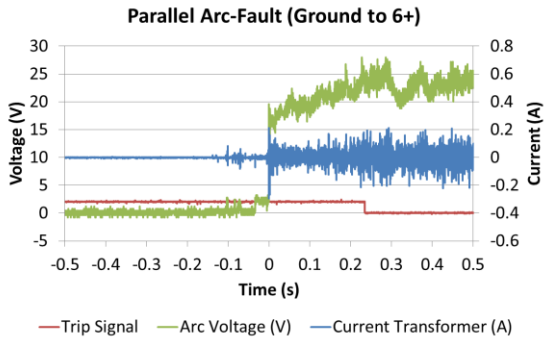

Fig. 10. Parallel arc-fault current and voltage. Trip time was 235 ms.

III. DIFFERENTIATION OF SERIES AND PARALLEL ARC-FAULTS

As shown above with the load bank and inverter tests, discriminating parallel and series arc-faults is not possible using the string frequency noise alone. Instead, additional diagnostic sensors must be employed. Here we present three methods to classify series or parallel arc-faults. This may be necessary in order to take the appropriate action to de-energize the different arc-faults.

Method 1: Use a combination of arc-fault high frequency noise along with changes in current or voltage. First suggested by Strobl and Meckler [8], parallel arc-faults are often associated with a drop in current and voltage to the inverter or charge controller (see Figs. 7 and 9), whereas series arc-faults show little change in current or voltage on the string (see Fig. 4). Based on the experimental work presented here, these drastic current and voltage changes are unlikely to exist from irradiance changes. However, in order to prevent false diagnoses, a combination of arcing noise with a change in the current and voltage is recommended. One potential problem with this method is that if the inverter shuts off during a parallel arc-fault, the arcing frequencies may not reach the arc-fault detector and it would appear as though the system was safely de-energized when, in fact, a parallel arc-fault is still burning.

Method 2: Force the PV array to V_{oc} and recheck arc-fault noise. By pushing the arcing string off its maximum power point (MPP), series arc-faults would be extinguished but parallel arc-faults would continue. This could be done with the inverter MPP Tracker adjusting the system toward V_{oc} or by physically inserting a resistance (R_1) in the string. With the additional resistance in the circuit, there is less current available to sustain the series arc-fault, illustrated in Fig. 11. With enough impedance, the current will drop enough that the series arc-fault will be extinguished but a parallel arc-fault will not, so by rechecking for arc-fault frequencies with R_1 in the circuit, a parallel arc-fault would be identified. Maintaining the continuity of the circuit is critical to ensure the arc-fault frequencies still reach the arc-fault detector. Opening the circuit prevents the noise from propagating through the array, thereby eliminating the possibility to recheck the system for parallel arc-fault noise. Parallel arc-fault noise is indistinguishable from baseline noise when the array is open, shown in Fig. 12.

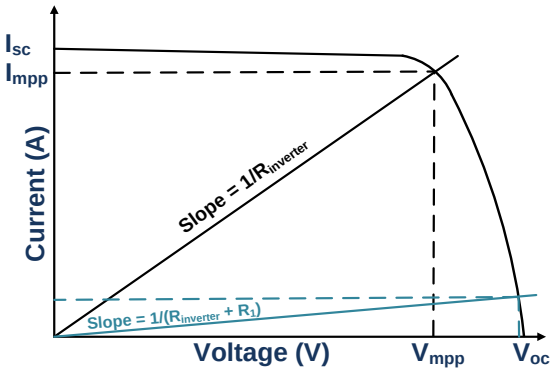

Fig. 11. Operation of the PV system normally and with high series resistance.

The resistance, R_1, required to extinguish the series arc-fault will depend on the system. Experimental work with the load bank showed that for a system with R_{mpp} = ~50 Ω, $R_{inverter} + R_1$ = 225 Ω could sustain the arcs but at 450 Ω, the arc-fault was difficult to sustain. At this same resistance, the parallel arc-fault noise was easy to identify. The increase in resistance can be performed with the inverter adjusting the MPP and would add no additional costs to the PV system.

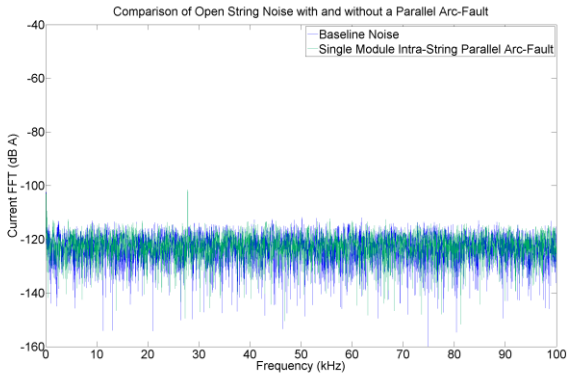

Fig. 12. Baseline and intra-string parallel arc-fault noise. Parallel noise is not present when the string is open.

Method 3: Permanently connect parallel strings to establish a noise path to the AFD. When two or more PV strings are connected using T-branch connectors or solid connections at the combiner box, a loop in the PV system allows the arc-fault noise to reach the arc-fault detector even when the DC disconnect at the combiner box or inverter is open. When the disconnect is open, parallel arc-fault noise will reach the arc-fault detector but series arc-faults will be extinguished. An illustration of the configuration is shown in Fig. 13. An example of parallel arc-fault noise with the disconnect open is shown in Fig. 8. Thus, series and parallel arc-faults could be differentiated and de-energized using the procedure:

1. When arc-fault noise is detected, open the DC disconnect. (This de-energizes any series arc-fault.)
2. If the noise persists, the arc-fault noise is from a parallel arc-fault and appropriate action can be taken.

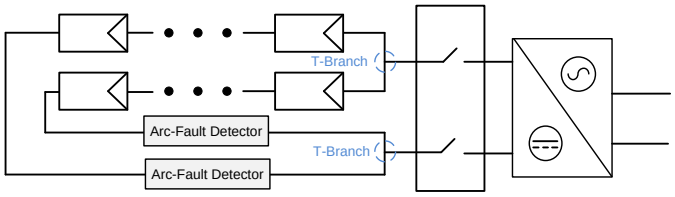

Fig. 13. Method for series arc-fault to be extinguished, but parallel arc-faults to remain active and detectable by the arc-fault detector.

Since this method guarantees series arc-faults will be extinguished quickly with the opening of the dc disconnect(s), it may be superior to Method 2.

IV. PARALLEL ARC-FAULT DE-ENERGIZATION

In order to de-energize a series arc-fault, it is fairly straightforward: the string must be opened at one or more locations to prevent current flow to the arc. Unfortunately, the mitigation routine for parallel arc-faults is less obvious. There are two leading theories on how to extinguish parallel arc faults: open connectors between each module or short the array. As shown in Table II, either opening or shorting the array will extinguish the parallel arc-fault cases listed in Fig. 1. Opening the connectors between each module limits system voltages to the open circuit voltage of a single module. Shorting the string or each module effectively drops all the conductors to 0 V ground potential and pushes the module operating points toward I_{SC}, where there is no voltage between conductors. Without the gap voltage the parallel arc-fault will be extinguished. This was confirmed at DETL by extinguishing parallel arc-faults (i) on a string of three modules with an arc-fault across the middle module and (ii) on a string of seven modules with an arc-fault from Modules 2 to 6. In both cases repeated parallel arc-faults with the string open were immediately extinguished when the string was shorted.

In the case of a parallel arc-fault within a module, shown in Fig. 14, opening the connectors (arrows) would not de-energize the arc and the fault would continue with a gap voltage of $V_{OC}/3$. V_{OC} for many modern modules is well above 50 V so opening the connectors between the modules would not reduce the voltage to a level which ensures arc-fault suppression (~12 V).

Shorting the array or modules is not without its limitations though. One concern with shorting portions of an active array is the energy conducted through the switch could be high due to the charge stored on the input capacitor of the inverter. To prevent the capacitor energy from dumping into the system, an additional series switch could be used to disconnect the inverter, but this adds complexity and cost, and slows the system response. Also, servicing an array that has been shut down by shorting poses a challenge, as there is no reliable way to eliminate current flowing through the string conductors. Additionally, the shorting switch cannot be opened without reestablishing the conditions for the arc-fault. The only safe way would be to disconnect the string wiring when the array is not exposed to sunlight, which would delay a full system shut down.

Tigo Energy notes that there is considerable overlap in the electronics required for the DC optimization of a module's operating characteristics and an arc-fault detector. For a

TABLE II
PARALLEL ARC-FAULT PROTECTION OPTIONS

Parallel Arc-Fault Location	***De-energization via Opening Between Modules?***	***De-energization via Shorting Between Modules?***	***De-energization via Shorting the String?***
To grounded conductor	Yes	Yes	Yes
Cross-string	Yes	Yes	Yes
Intra-string	Yes	Yes	Yes

nominal additional cost, a detector could be integrated into each junction box. Then any module that detects an arcing signature could independently respond by opening the module's output, which would immediately reduce the total power available to sustain the arc-fault. Once the arc-fault is extinguished, a central processor could collect the data from the individual modules, analyze the results for arc-fault patterns, and make a determination of whether a series or parallel arcing has occurred. This processor could also safely shut down the remainder of the array and provide notification that an event has occurred

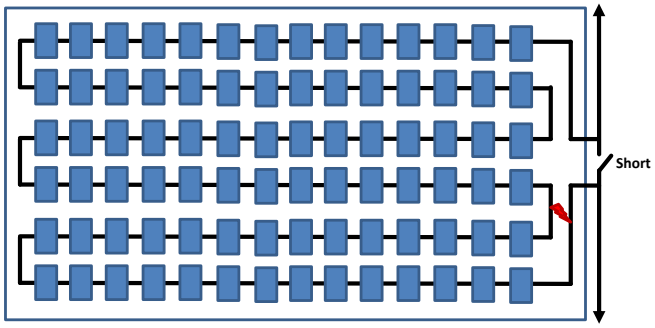

Fig. 14. High power PV module with internal arc-fault.

If parallel arc-fault protection is adopted in the 2014 *NEC*, the *Code* will not state the method in which the parallel arc-faults should be de-energized—simply that they must be. Individual arc-fault circuit interrupter manufacturers will need to determine the safest way to eliminate series and parallel arc-fault hazards.

IV. CONCLUSIONS

Arc-fault detectors designed to satisfy *National Electrical Code* 690.11 often use the frequency content of the PV DC system to determine when a series arc-fault is established. Unfortunately this method does not provide a means for differentiating series and parallel arc-faults because the arc-fault noise is similar for both arc-fault types. We present three alternative methods for differentiating parallel and series arc-faults and recommendations for the suppression of both arc-fault cases. Once the arc-fault type is determined, series arc-faults can be de-energized by opening the string at any point. Many parallel arc-faults can be de-energized by opening connectors between the modules and all parallel arc-faults can be de-energized by shorting the modules or the strings. Unfortunately, the shorting solution requires shorting the input capacitor of the inverter and repairs to the array would require shading the modules or working at night. Additional analysis of different system configurations and appropriate AFCI responses during parallel arc-fault events is recommended.

ACKNOWLEDGEMENT

Sandia National Laboratories is a multi-program laboratory managed and operated by Sandia Corporation, a wholly owned subsidiary of Lockheed Martin Corporation, for the U.S. Department of Energy's National Nuclear Security Administration under contract DE-AC04-94AL85000. This work was partly funded by the US Department of Energy Solar Energy Technologies Program and partly supported by the National Renewable Energy Laboratory under subcontract NEU-2-11979-03.

REFERENCES

[1] National Electrical Code, 2011 Edition, NFPA70, National Fire Protection Association, Quincy, MA.
[2] B. Brooks, The Bakersfield Fire, SolarPro 4.2, Feb/Mar 2011.
[3] B. Brooks, Report of the Results of the Investigation of Failure of the 1.1135 MW Photovoltaic (PV) Plant at the National Gypsum Facility in Mount Holly, North Carolina. Brooks Engineering Draft Report. 26 May, 2011.
[4] A. Schlumberger, A. Kreutzmann, Brennendes Problem – Schadhafte BP-Module können Feuer entfachen, Photon, August 2006, pp. 104-106 (in German).
[5] T. Zgonena, L. Ji, and D. Dini, Photovoltaic DC Arc-Fault Circuit Protection and UL Subject 1699B, Photovoltaic Module Reliability Workshop, Golden, CO, Feb. 2011.
[6] J. Johnson and W. Bower, "Codes and Standards for Photovoltaic DC Arc-Fault Protection," Presentation for Solar American Board for Codes and Standards, Dallas, TX, 21 Oct., 2011.
[7] J. Johnson, B. Pahl, C.J. Luebke, T. Pier, T. Miller, J. Strauch, S. Kuszmaul and W. Bower, "Photovoltaic DC arc fault detector testing at Sandia National Laboratories," 37th Photovoltaic Specialists Conference, Seattle, WA, 19-24 June 2011.
[8] C. Strobl and P. Meckler, Arc Faults in Photovoltaic Systems, *2010 Proceedings of the 56th IEEE Holm Conference on Electrical Contacts*, pp.1-7, 4-7 Oct. 2010.
[9] H. Haeberlin, Arc Detector as an External Accessory Device for PV Inverters for Remote Detection of Dangerous Arcs on the DC Side of PV Plants, European Photovoltaic Solar Energy Conference Valencia, Spain 2010.
[10] S. Bieniek, H. Behrends, G. Bettenwort, T. Bülo, A. Häring, M. Hopf, M. Kratochvil, C. Merz, T. Wegener, Fire prevention in PV plants using inverter integrated AFCI, 26th European Photovoltaic Solar Energy Conference and Exhibition, Hamburg, Germany, 2011.
[11] A. Häring and S. Bieniek, "Prevention and Detection of Arc Faults in PV Systems," Photon's 2nd PV Safety Conference, 2011, Berlin, Germany
[12] H.-L. Tsai, C.-S. Tu, and Y.-J. Su. "Development of Generalized Photovoltaic Model Using MATLAB / SIMULINK," Proceedings of the World Congress on Engineering and Computer Science, 2008, pp. 0-5.
[13] J. Worden and M. Zuercher-Martinson, How Inverters Work: What Goes on Inside the Magic Box, SolarPro, Apr/May 2009.
[14] R.F. Ammerman, T. Gammon, P.K. Sen, and J.P. Nelson, DC-Arc Models and Incident-Energy Calculations, IEEE Transactions on Industry Applications, Vol. 46, No. 5, pp.1810-1819, September-October 2010.
[15] Underwriters Laboratories (UL) Subject 1699B, Outline of Investigation for Photovoltaic (PV) DC Arc-Fault Circuit Protection, April 29, 2011.